https://doi.org/10.1017/S1551929510000404 Published online by Cambridge University Press

Enhanced Detection Sensitivity with a New Windowless XEDS System for AEM Based on Silicon Drift Detector Technology

P. Schlossmacher,* D.O. Klenov, B. Freitag, and H.S. von Harrach
FEI Company, Achtseweg Noord 5, P.O. Box 80066, 5600 KA Eindhoven, The Netherlands
* peter.schlossmacher@fei.com

Introduction

For many years now, the combination of the modern S/TEM system (scanning/transmission electron microscope) with the X-ray energy dispersive spectrometer (XEDS) has resulted in Analytical Electron Microscopes (AEMs) able to deliver both high-resolution imaging and elemental composition maps in the same instrument. This ability to correlate local elemental composition with microstructure has greatly broadened the applications realm of the S/TEM instrument. The boundaries of performance for many of these applications are now determined by limits in XEDS system detection sensitivity. In this article, we describe an AEM with greatly enhanced detection sensitivity due to a number of innovations in the system architecture, including: a high-brightness Schottky FEG source, four detectors integrated deeply into the objective lens, windowless silicon drift detector technology with shutters, and high-speed electronics readout. This new system architecture provides many performance benefits, such as improved light element detection, better sample tilt response, faster mapping, and especially enhanced system detection sensitivity.

AEM System Architecture

Silicon Drift Detectors (SDDs) are rapidly replacing Si(Li) detectors for XEDS in SEMs, but they only recently began entering the S/TEM world. One of the biggest advantages of SDDs is their capability of handling very high count rates, which can easily be generated with bulk samples in an SEM; such count rates are seen as less likely or even impossible with thin specimens in the S/TEM. However, the advent of probe-corrected S/TEMs and high-brightness Schottky field emission sources (X-FEGs)—the latter refers to the implementation described in this paper—has led to a considerable increase in available beam currents even in small electron probes, and therefore much higher XEDS count rates are now achievable. Moreover, SDDs can be designed in a very compact way allowing the integration of multiple detectors inside the S/TEM column as opposed to just attaching them to ports close to the objective lens. A first implementation of such a design in a new 200 kV S/TEM system, the Tecnai Osiris™ [1], was recently presented [2, 3]. Four SDDs designed by PN Sensor were symmetrically placed around the optical axis close to the sample area (see Figure 1). A total sensor area of 120 mm^2 and its integration deep inside the electron-optical column result in a solid angle of 0.9 steradian (sr), which is the largest solid angle implemented so far in a commercial S/TEM system. The four SSDs are cooled for optimum performance by a direct connection to the cold trap of the S/TEM. The detector system and cold trap share the same dewar, which offers a capacity for more than 4 days of liquid nitrogen supply. The windowless design of the SDDs improves the sensitivity for light elements compared to detectors with thin polymer windows, and mechanical shutters protect the SDDs against high-energy electrons at low magnifications.

Specially designed front-end electronics and an ultra-fast multi-channel pulse processor are provided by Bruker AXS in collaboration with FEI [2, 3]. The entire XEDS system is fully embedded in the system control of the S/TEM system. Pixel dwell times down to 10 µs can be used for fast mappings, acquired and processed using Bruker's ESPRIT software [2, 3].

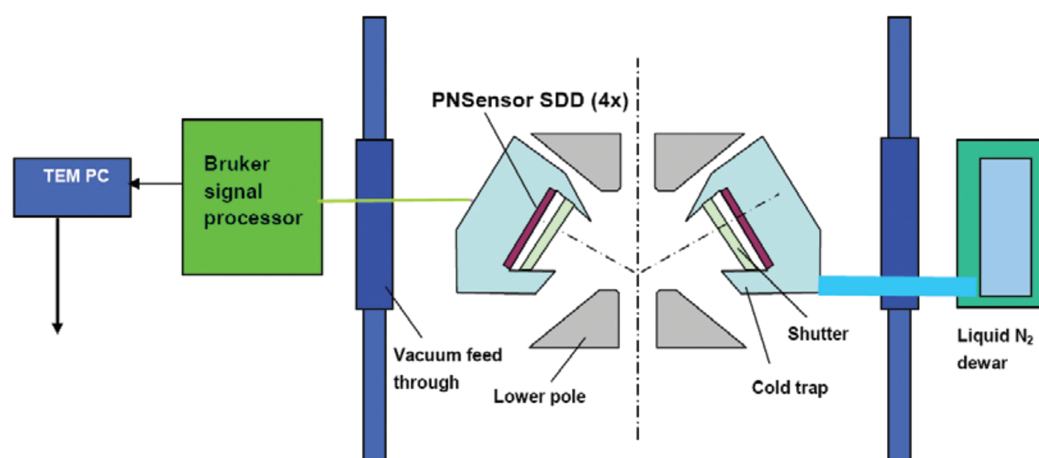

Figure 1: Schematic drawing of the Super-X design viewed as a cross section through the objective lens and specimen. Two of the four X-ray detectors are shown mounted on the cold trap surrounding the specimen (see text for details).

The novel ChemiSTEM™ technology on the Tecnai Osiris comprises this new proprietary XEDS detector system (Super-X design) in combination with a high-brightness Schottky field emission electron source (X-FEG) as the two major components. It is the combination of a significantly enhanced generation of X-rays by an increased beam current with the enhanced detection efficiency of the new detector system that delivers an improved performance in XEDS analytics.

 doi: 10.1017/S1551929510000404

Put the Knowledge and Experience of an EDS Expert to Work for You

...and Change the Way You do Analysis Forever

B Kα, Si Kα...5 kV...ZAF > X?

EDAX Introduces the New TEAM Analysis System–

Smart Features at Your Fingertips:

Smart Track – An Environmental Status Panel provides system data, monitors it, and notifies you of operating conditions for your detector, stage, column, and more

Smart Acquisition – Routine tasks can be automated, allowing you to make the most efficient use of your time

Smart Mapping – Map your sample immediately and obtain a complete elemental and phase analysis

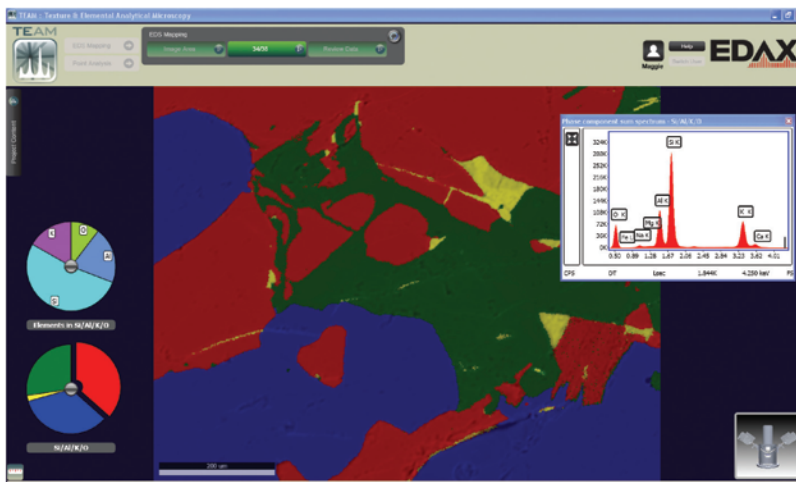

TEAM Up with EDAX for SMART EDS Analysis.
Visit our website at www.EDAX.com/TEAMSMART
or call 1-201-529-4880.

AMETEK®
MATERIALS ANALYSIS DIVISION

Visit Us at M&M Booth 875

EDAX®
advanced microanalysis solutions

https://doi.org/10.1017/S1551929510000404 Published online by Cambridge University Press

https://doi.org/10.1017/S1551929510000404 Published online by Cambridge University Press

Examples of this performance are presented in the following sections.

Practical Advantages of the XEDS Design

Clearly, a major advantage comes from the large solid angle for X-ray collection provided by four X-ray detectors symmetrically arranged around the specimen. There is also an important advantage related to specimen tilting. The dependency of the detected X-ray count rate on the specimen tilt is greatly improved compared to a standard single XEDS detector. Figure 2 shows measurements of the new XEDS system count rates over a tilt range from –25° to +25°. The count rate measured at 200 kV using a commercially available NiO_x film with a nominal thickness of 50 nm ± 10 nm [4] never drops below 80% of the maximum count rate over this tilt range. Moreover, it should be noted that the maximum count rate is achieved at zero degree tilt. In contrast, a single detector solution, whether Si(Li) or SDD, always suffers from its asymmetrical geometrical placement. Count rate is maximized only when tilting towards the (single) detector and strongly decreases when the orientation of the sample requires negative tilt angles, for example, at an interface or grain boundary. For negative tilt angles above -10°, the count rate even drops to zero in most conventional XEDS systems because the sample and/or specimen holder completely shadow the single detector. Figure 2 also shows an example of this single detector tilt dependency on a conventional XEDS system with a 0.3 sr solid angle.

Materials science problems in thin film technology and in grain boundary studies often require imaging in an edge-on orientation, which cannot be established without sample tilting. In that edge-on orientation, XEDS maps or line scans across the interfaces must be acquired to get the desired information. On the other hand, investigations of small nanoparticles, for example, in catalysis or in the synthesis of new materials, bear the risk of losing a specific particle when a certain sample tilt has to be applied for optimum XEDS detection. The ability to acquire high XEDS count rates irrespective of sample tilt adds a new degree of flexibility to any analytical/imaging problem to be solved with AEMs.

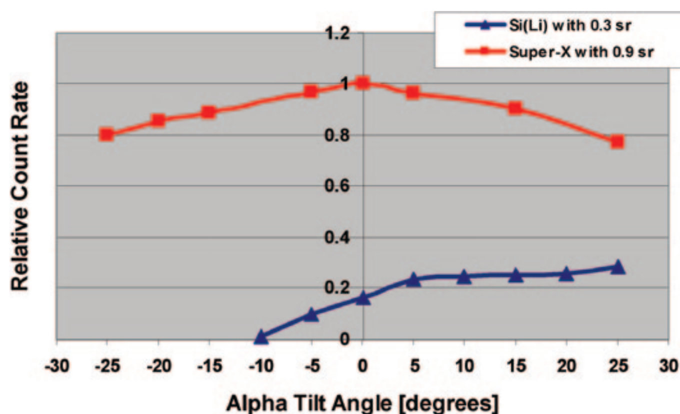

Figure 2: Comparison of relative XEDS count rates of the Super-X (0.9 sr) and a standard Si(Li) detector with 0.3 sr solid angle. Both TEM/STEMs were operated at 200 kV with the same (constant) beam current. NiO_x films were used as samples for both tilt series. Positive tilt angles represent specimen tilts towards the single detector.

How to Compare Different Detector Systems?

Figure 2 also reveals that the difference in detection efficiency is not just due to the larger solid angle and the four-detector geometry. Comparing the count rates at optimum tilt angle for each XEDS system, one expects the difference to be a factor of 3, which equals the ratio in the solid angles. At their optimum tilt angles, however, the two systems differ by a factor of approximately 4, and by a factor of 5 when both are compared at zero tilt angle.

An explanation for the discrepancy factor of 4 at optimum tilt angle lies in the fact that all commercially available XEDS detectors, Si(Li) as well as SDDs, use a thin polymer window. These windows are supported by a rigid silicon grid (380-µm thick), which leaves open only 77% of the detector area [5]. Therefore, calculating the solid angle by taking the full detector area and neglecting the effect of the silicon grid leads to an overestimation of the solid angle by about 43%.

Other often unknown parameters are important to judge detection geometries and efficiencies: detector elevation angle, distance from detector to sample, sample holder geometry, and others. Some of these parameters cannot be measured by users because they depend on proprietary design drawings or on the specific implementations/geometries in combination with a certain S/TEM column. Users have no chance to fairly compare these numbers. Therefore, only raw solid angles or even raw detector areas are compared, which does not give the full picture, as seen in Figure 2.

To more objectively measure the detector efficiency of an XEDS system without knowing these geometrical details, the following procedure is proposed: take a sample of known thickness (which can be quantified for example by EELS) and measure the XEDS count rate per applied beam current. Measuring the number of X-ray input counts per second for a given beam current takes into account the whole geometry including potential shadowing by the sample holder.

In Figure 3, input counts per second (cps) are plotted as a function of beam current for two different AEM systems: a 200 kV S/TEM with Schottky-FEG and Si(Li) detector of 0.3 sr solid angle (in blue) and the Tecnai Osiris with ChemiSTEM technology and 0.9 sr solid angle (in red). The small inset shows the lower-left part of the plot in more detail. In both experiments the same FIB-cut InP sample was used, and the counts were integrated over the full energy range. In order to be sure that all measurements were taken on sites of the same thickness, EELS was employed to control sample thickness by measuring t/λ (thickness in relation to average mean free path). Figure 3 displays the measured input counts versus incident beam current as solid lines together with calculations of the respective output counts, taking into account the effect of electronics system dead time. The first observation from this figure is that the new system acquires more than five times the X-ray counts per second per nanoampere beam current compared to a the standard S/TEM-AEM, even when equipped with a 0.3 sr Si(Li) detector. Secondly, more than 15 times higher beam currents can be applied in the case of the X-FEG plus new Super-X XEDS system. Third, much higher total counts (input as well as output) can be achieved using the X-FEG/Super-X combination.

High Definition Digital
TEM Cameras with
1 to 16 Megapixels

- AMT SOLUTIONS
- Life Science Cameras
- Material Science Cameras
- Easy To Use Software
- Reliability and Services
- TEM Integration
- Extensive Support

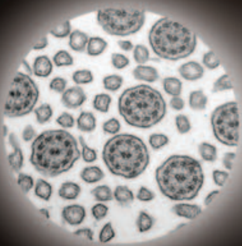
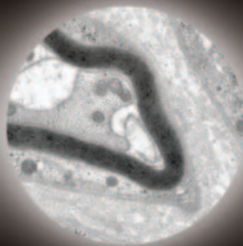
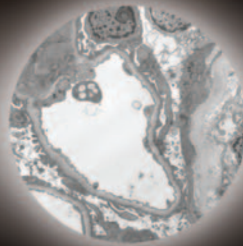
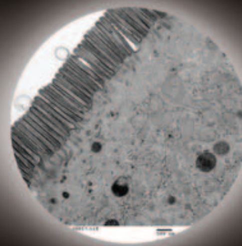
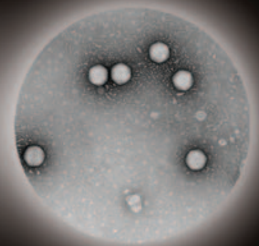

3 Electronics Avenue, Danvers, MA 01923 • Phone: 978.774.5550 • www.amtimaging.com

https://doi.org/10.1017/S1551929510000404 Published online by Cambridge University Press

https://doi.org/10.1017/S1551929510000404 Published online by Cambridge University Press

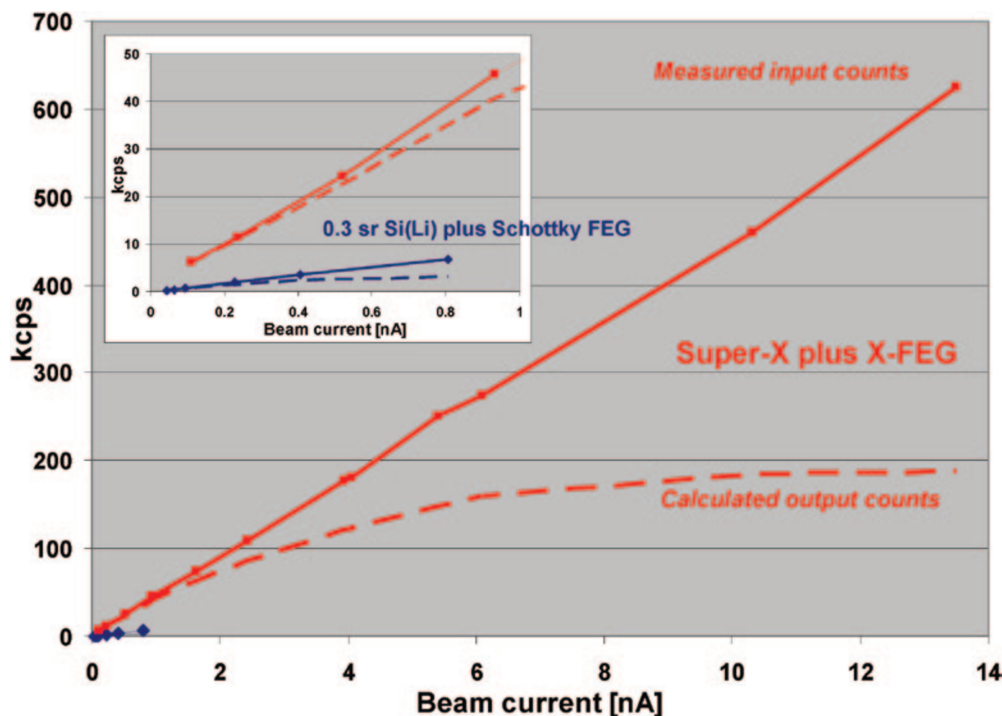

Figure 3: Plot of measured total X-ray counts per second (solid lines) as a function of beam current for two different systems: a 200 kV TEM with Schottky-FEG and Si(Li) detector offering 0.3 sr solid angle (in blue) and the Tecnai Osiris equipped with X-FEG and Super-X detector with 0.9 sr (in red). Solid lines represent the experimental values based on input counts; broken lines refer to calculations of output counts taking into account dead time. In both experiments the same FIB-cut InP sample was used with a thickness of about 200 nm.

close to 0.3 nm. This data set was acquired in 100 minutes using multiple frames, 1-nA beam current, 50-µs dwell time, and drift correction. The short pixel dwell time of 50 µs was necessary in this case to avoid sample damage. Besides a HAADF-STEM and an overlay image of various elements (upper half), Figure 5 also displays a number of elemental maps of selected elements with quantifiable integrated intensities. The acquisition time of 100 minutes was chosen to achieve good statistics in each, which then permits full quantification pixel-by-pixel without binning using built-in routines of Bruker's Esprit software based on Cliff-Lorimer factors. Contrast in elemental maps is proportional to the concentration from 0 to 100% over 256 intensity levels. Special attention should be paid to the thin layers of Ta and Hf, which can be clearly identified

Sensitive Detection of Light Elements

The detection of light elements is not regarded as the main domain of XEDS. The combination of SDD technology with a windowless design considerably enhances the sensitivity for light elements like oxygen and nitrogen, as displayed in Figure 4. A silicon multilayer sample was investigated at 200 kV, and elemental maps were recorded with 0.8 nA beam current in the Tecnai Osiris. All elemental maps are 350 × 50 pixels in size and were acquired simultaneously by XEDS in 60 seconds. The oxygen and nitrogen maps clearly allow distinction between SiO, SiON, and SiN, respectively; whereas the grayscale contrast of the HAADF-STEM image does not permit the same. The Z-contrast of the STEM image is not sensitive enough to visualize the compositional difference between SiO, SiON, and SiN layers.

Fast Mapping of Large Areas

Because of the capabilities of the new XEDS system (including fast electronics), elemental maps can be recorded with mapping speed enhancements of factors up to ~50 when benchmarked against the 0.3 sr XEDS Si(Li) system shown in Figure 3. The new system software allows map sizes up to 1,000 × 1,000 pixels to be collected as spectrum images. This means that a full spectrum (in this case up to 80 keV: 4096 channels with up to 20 eV/channel) may be acquired and stored at each image pixel. This allows post-acquisition searching for further elements in the stored data cube.

Figure 5 shows a 45-nm PMOS transistor structure as an example of a large map with 600 × 600 pixels. The full image width is ~190 nm, which corresponds to a pixel resolution of

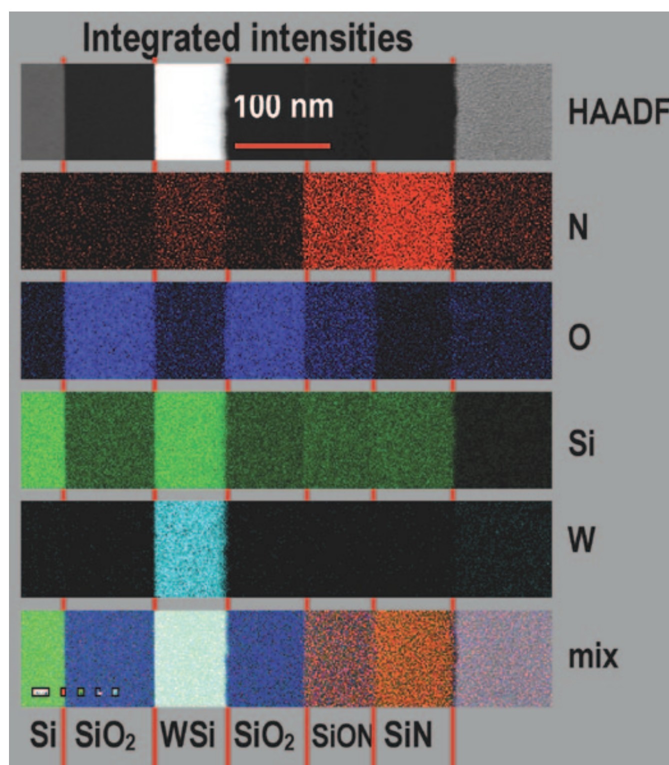

Figure 4: HAADF-STEM image and XEDS elemental maps of a silicon multilayer structure. Each elemental map comprises 350 × 50 pixels and was recorded at 200 kV with a 50-µs dwell time and a beam current of 0.8 nA. About 60 frames were accumulated in 60 seconds. Specimen is courtesy of FELMI-ZfE (Graz, Austria).

https://doi.org/10.1017/S1551929510000404 Published online by Cambridge University Press

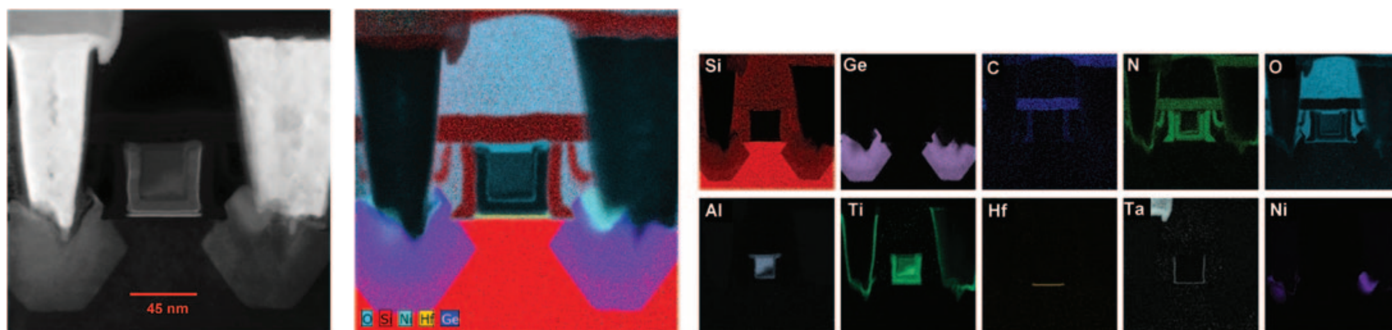

Figure 5: HAADF-STEM image and overlay elemental map of a 45-nm PMOS transistor structure are displayed in the upper half and 10 maps of different elements in the lower half of the figure. Each image/map comprises 600 × 600 pixels. Using a 50-μs pixel dwell time, 1-nA beam current, and drift correction, multiple frames were recorded and accumulated over a total acquisition time of 100 minutes. The width of the field-of-view is about 190 nm, which results in a pixel resolution of HAADF-STEM image and elemental maps of 0.3 nm.

although they are only about one nanometer in thickness. The presence of light elements like C, N, and O are imaged at high sensitivity, as already discussed in Figure 4. A map with this same pixel size and level of count statistics on the 0.3 sr conventional Si(Li) system of Figure 3 would have taken approximately 3 days of mapping time, which is not practical for a number of reasons such as throughput time, system drift, and sample integrity.

Detection of Low Concentrations

An example of the new system's high sensitivity is demonstrated by detection of elements that are present in low concentration (for example, ≤1 wt.%). Metals and alloys often contain elements in low concentration that can influence the mechanical properties. Fortunately, metals and alloys can withstand high beam currents in the order of 20–30 nA in a nanometer-sized probe without detectable damage. Such high currents permit mappings with many pixels and/or over large sample areas because pixel dwell times can be kept short. As a result XEDS maps with good counting statistics can be acquired in reasonable times.

Figure 6 shows the microstructure of a Ti-5553 alloy sample. The nominal composition is given as Ti-5Al-5Mo-5V-3Cr-0.5Fe (wt.%). Although the total Fe content is just 0.5 wt.%, the Fe distribution can be imaged over an area of almost 500 × 500 nm (100 × 100 pixels) in less than 4 minutes (225 s). These maps were produced using a beam current of 22 nA and a pixel dwell time of 10 ms. It should be noted that Fe could only be detected in the matrix and not in the TiAl laths (Fe-free regions). Because Fe and Co are sometimes observed as contributions from the pole piece material—so-called systems peaks—it is remarkable that no Fe signal was detected in the TiAl laths even though very high beam currents were applied. This demonstrates the cleanliness and high quality of the XEDS spectra of the new AEM system. The lower part of Figure 6 displays an XEDS spectrum from the entire map area. This spectrum contains about 20 million (output) counts after the total acquisition time of 225 seconds. The Fe

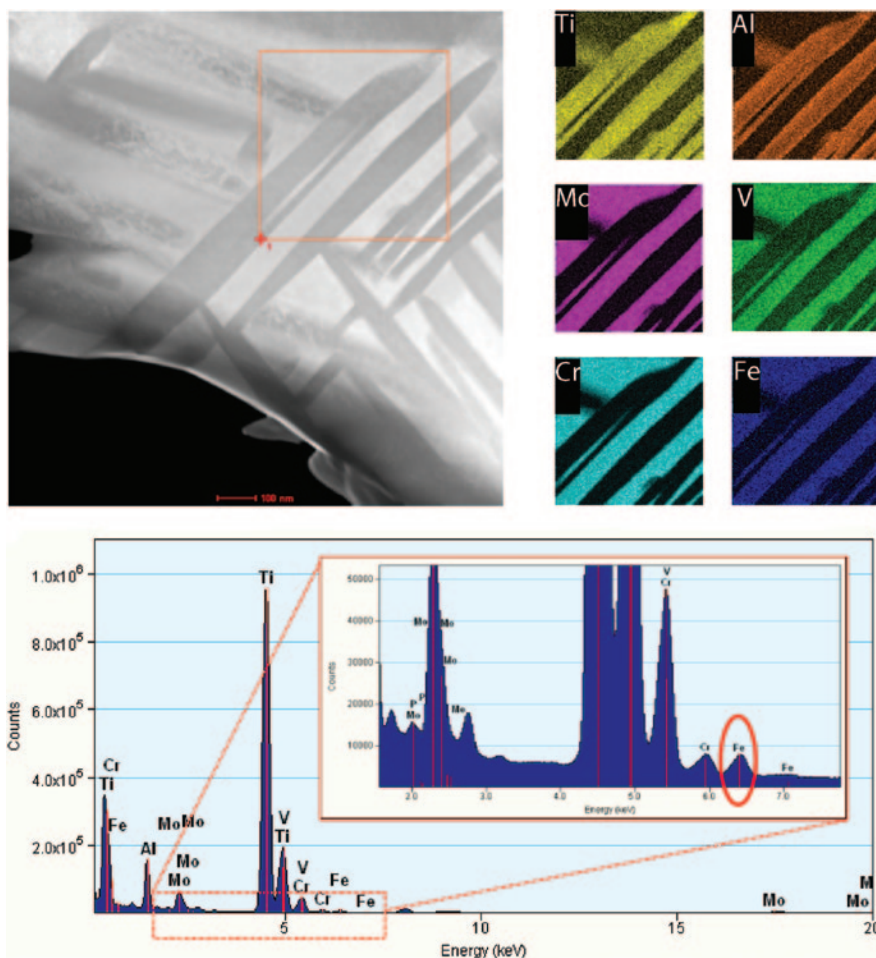

Figure 6: HAADF-STEM image of a TiAl laths structure in a Ti-5553 alloy (upper left). The nominal composition is given as Ti-5Al-5Mo-5V-3Cr-0.5Fe (wt.%). XEDS elemental maps of an area of about 470 nm × 470 nm, indicated by a red square in the HAADF-STEM image, (upper right) display the major constituent elements: Ti, Al, Mo, Cr, V, and Fe. Pixel size of the maps is 100 × 100, and the pixel dwell time is 10 ms. The lower part displays the integrated EDX spectrum of the entire mapped area; the insert is a magnified plot to show the Fe peak (red ellipse), which contains about 130,000 output counts including background. The specimen is courtesy of Dr. Pete Collins (Ohio State University; now at Quad City Manufacturing Laboratory, Rock Islands, IL).

https://doi.org/10.1017/S1551929510000404 Published online by Cambridge University Press

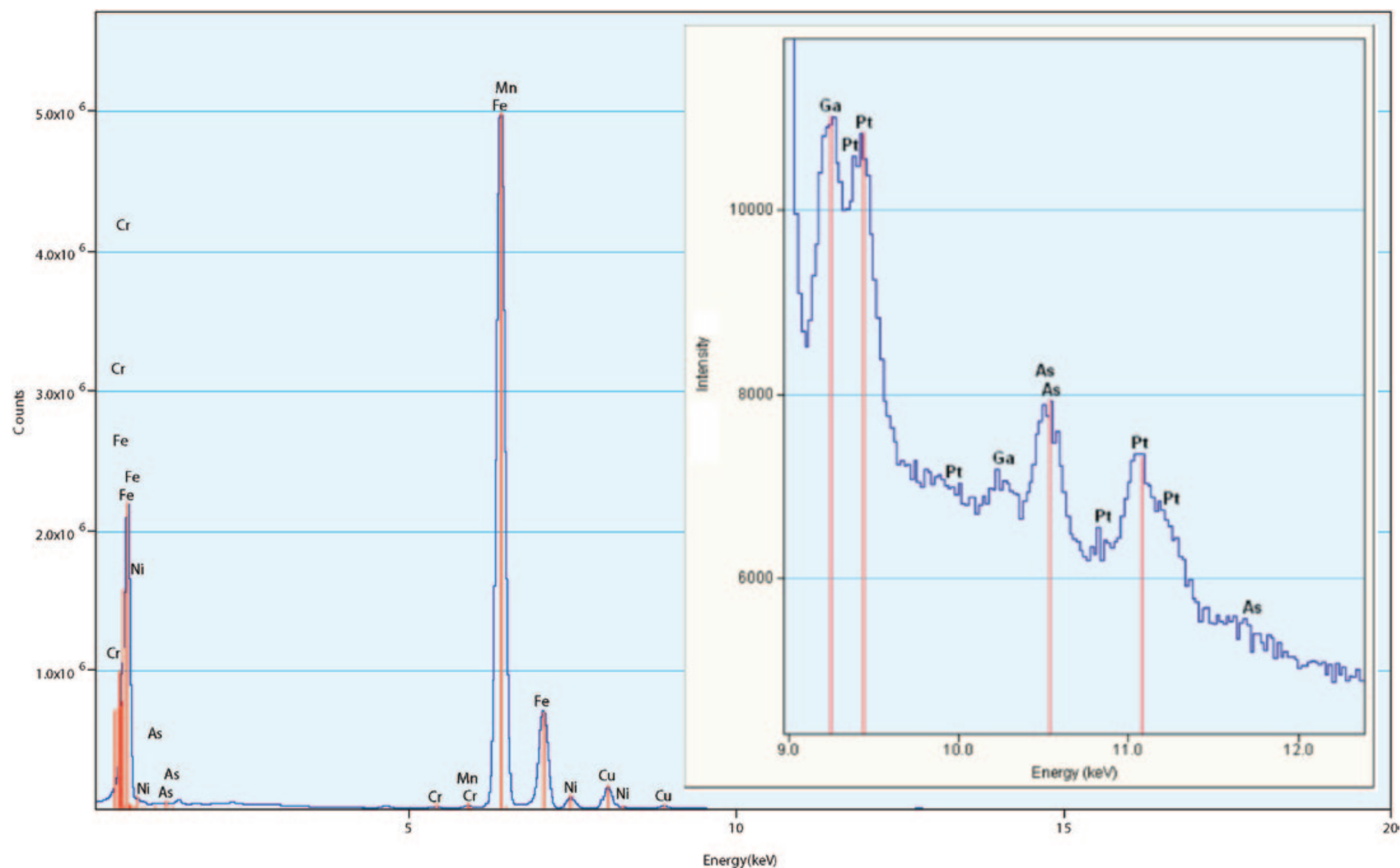

Figure 7: XEDS spectrum from 0–20 keV of the NIST steel standard No. 461. A large rectangular area was scanned with a 1.7-nA beam for 600 seconds. This NIST steel contains mostly Fe and a couple of impurities at low concentration, like As with 0.028 wt.%. The insert shows an energy range from 9 to 12 keV. The As-Kα peak at 10.5 keV is clearly visible above background and also Ga and Pt peaks, which stem from the FIB preparation process.

peak including background contains 130,000 (output) counts on a background of 70,000 counts. Applying a well-known formula [6] to calculate the minimum mass fraction (MMF) results in a MMF for Fe of 0.01 wt.%, assuming the nominal 0.5 wt.% of Fe as input.

Another example of the exceptional performance of this system is illustrated in Figure 7, which presents a spectrum from NIST steel standard (Standard Reference Material NBS No. 461). The full spectrum (0–20 keV) was acquired in 600 seconds using a beam current of 1.7 nA while scanning a micron-sized area in order to average the composition over the microstructure. In bulk, this low-alloy steel has a nominal As concentration of 0.028 wt%, and although this sample was prepared for TEM analysis using FIB, it is expected that minimal changes have resulted in the composition. The inset of Figure 7 reveals that the As peak at 10.5 keV is clearly visible above background together with a few Ga and Pt peaks from the FIB process.

Conclusion

The design of a new XEDS system was presented and application examples from a new AEM system equipped with a high-brightness Schottky FEG (X-FEG) were shown. The gain in sensitivity and data acquisition speed compared to standard systems is substantial and opens access to new experiments, which were seen as too time-consuming or even impossible based on previous system sensitivity limitations. The high speed can be traded for large pixel mappings or for fast acquisition of XEDS data with very good statistics. Light element detection was demonstrated as well as the capability to detect elements in very low concentrations. The latter indicates that the element detection limit (minimum mass fraction of an element) for XEDS in S/TEM systems can be significantly improved.

References

[1] http://www.fei.com/products/transmission-electron-microscopes/tecnai.aspx

[2] HS von Harrach et al., *Microsc Microanal* 15 (Suppl 2) (2009) 208.

[3] HS von Harrach et al., *Proceedings of EMAG 2009* (in print).

[4] Commercially available from Agar or Pelco based on the paper RF Egerten and SC Cheng, *Ultramicroscopy* 55 (1994) 43.

[5] http://www.moxtek.com/PDF/Windows/AP3%20Windows.pdf. At X-ray energies above 10 keV, the Si grid becomes partially transparent for X-rays.

[6] M Watanabe and DB Williams, *Ultramicroscopy* 78 (1999) 89.

MT

https://doi.org/10.1017/S1551929510000404 Published online by Cambridge University Press

Side-By-Side Comparison? Difficult When Our Coaters Stand Alone.

High Resolution Sputter Coater 208HR for FE-SEM

Superior Features:

- High Resolution Fine Coating
- Wide Choice of Coating Materials
- High Resolution Thickness Control
- Multiple Sample Stage Movements
- Wide Range of Operating Pressures
- Compact, Modern, Benchtop Design

Find out about our complete line of sample coaters.

TED PELLA, INC.
Microscopy Products for Science and Industry

4595 Mountain Lakes Blvd., Redding, CA 96003-1448
Phone: 530-243-2200 or 800-237-3526 (USA) FAX: 530-243-3761
Email: sales@tedpella.com Web Site: www.tedpella.com